
The November 1999 Duzce Earthquake: Post-Earthquake Investigation of the Structures on the TEM

Publication No. FHWA-RD-00-146

Hamid Ghasemi, James D. Cooper, Roy Imbsen,
Hasan Piskin, Fulya Inal, and Azmi Tiras

Almost 3 months after the devastating Kocaeli earthquake of August 17, 1999, another earthquake with a moment magnitude of 7.2 hit Turkey on November 12, 1999. Called the Duzce earthquake, it caused nearly 1,000 fatalities and 5,000 injuries. The damage to buildings was similar to that sustained during the Kocaeli earthquake. Two viaducts and one tunnel under construction exhibited extensive damage.

The contents of this report are based on a reconnaissance survey of bridge and tunnel sites along the Trans-European Motorway (TEM) segment under construction near Bolu, conducted by the Federal Highway Administration (FHWA) team dispatched to Turkey on November 28, 1999. During this survey: (1) the roadway alignment and the physical condition of Bolu Viaducts #1 and #2 and Bolu Bridge #2 were observed; (2) superstructure damage to Viaduct #1 was viewed from both abutments and from atop Piers #4, #5, and #10 (the first expansion joint from the western abutment of the westbound span); (3) Damage to Bolu Bridge #2 was viewed from the west abutment seat and from atop the first pier east of the western abutment of the eastbound span; and (4) The Bolu Tunnel was inspected from the Elmalik portal westward to the collapse.

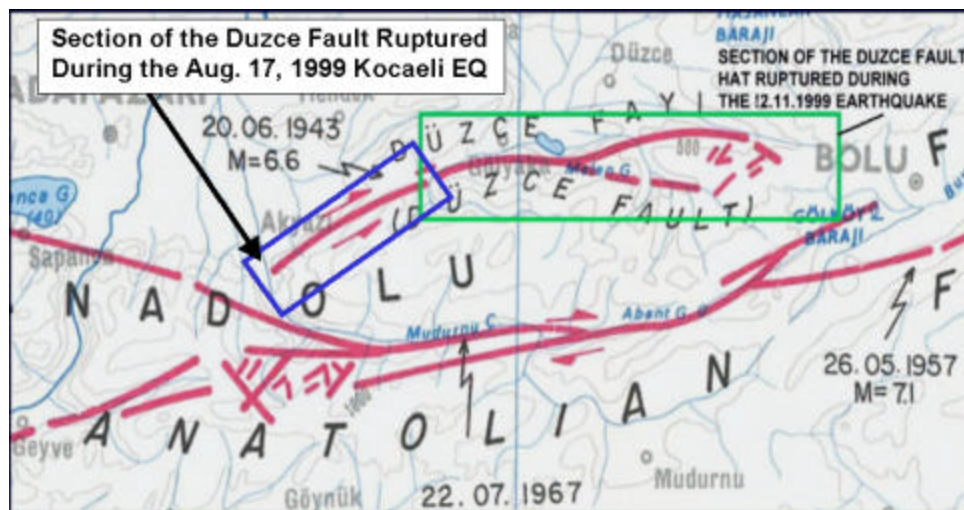
Introduction

The November 12, 1999 Duzce earthquake was caused by a right lateral strike-slip rupture along a significant part of the secondary Duzce fault near the town of Duzce (Figures 1 and 2). The length of the surface fault rupture is estimated to be 40 km, with an average lateral offset of 4 m along most of its length. The remaining part of the Duzce fault was ruptured earlier during the Kocaeli earthquake. According to seismologists the rupture on November 12 resulted from the stress created by the Kocaeli earthquake.

At the Duzce ground motion station near the epicenter, a Peak Ground Acceleration (PGA) of 1.0g was recorded before the ground-motion instrumentation was clipped (ceased functioning due to limitations on recording accelerations above 1.0g); at the Bolu station (30 km away) a PGA of 0.8g was recorded. The General Directory of Disaster Affairs operates these recording stations. Between the two stations, in the towns of Kaynasli and Bolu, there are two viaducts (Viaducts #1 and #2) and one tunnel (Bolu Tunnel) under construction. Therefore, it is reasonable to assume that these structures, which were not instrumented, experienced a PGA in excess of 0.4g, their design value. These structures are part of the last 24-km segment of the TEM that is to be completed. Figures 3 and 4 show this segment and a general view of the area with its



Figure 1. Map showing the epicenter of the Duzce earthquake and approximate location of the NAFZ.



<http://www.koeri.boun.edu.tr/earthqk/duzce4.html>

Figure 2. Map showing the ruptured sections of the Duzce fault.

mountainous terrain respectively. Viaducts #1 and #2, and the Bolu Tunnel located in this segment perhaps represent the most difficult part of the design and construction due to the close proximity of the Duzce fault and varied geological conditions.

The survey of this segment after the Duzce earthquake indicated that the considerable damage to the superstructure of Viaduct #1 and the Bolu tunnel was due to the near-fault effect. A surface fault trace was visible between the viaduct's piers and evidence of high-velocity impulses was observed from the earthquake records and at the sites. There are indications that high-velocity impulses or “fling” effects normal to the rupture of strike-slip faults are produced by the near-field effects of earthquakes, which present special problems for highway structures and tall buildings. These problems are manifested by very large displacements, overturning moments, the occurrence of liquefaction, and other energy-sensitive structural responses.

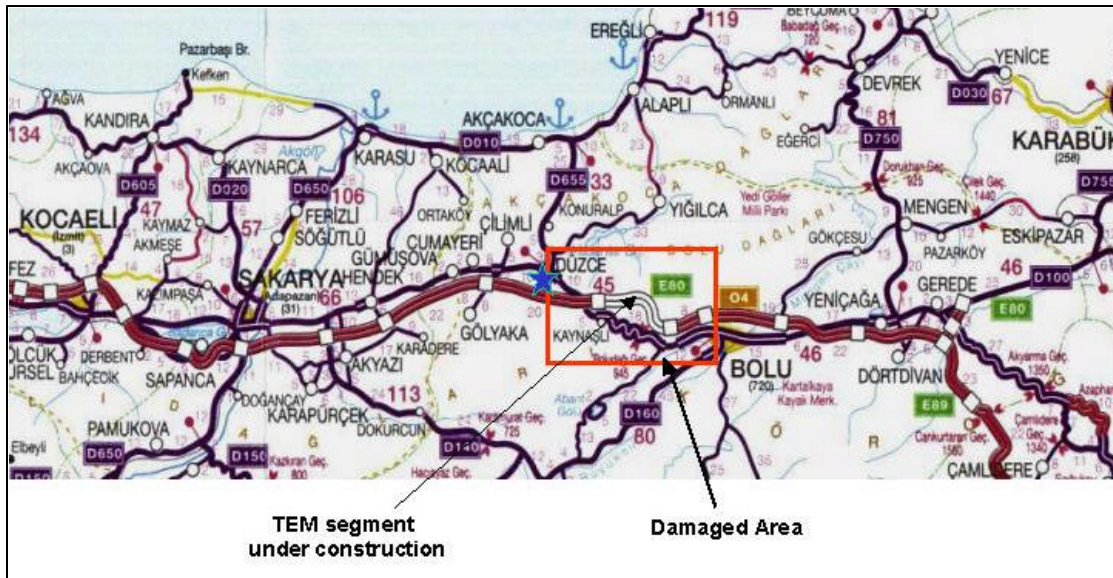
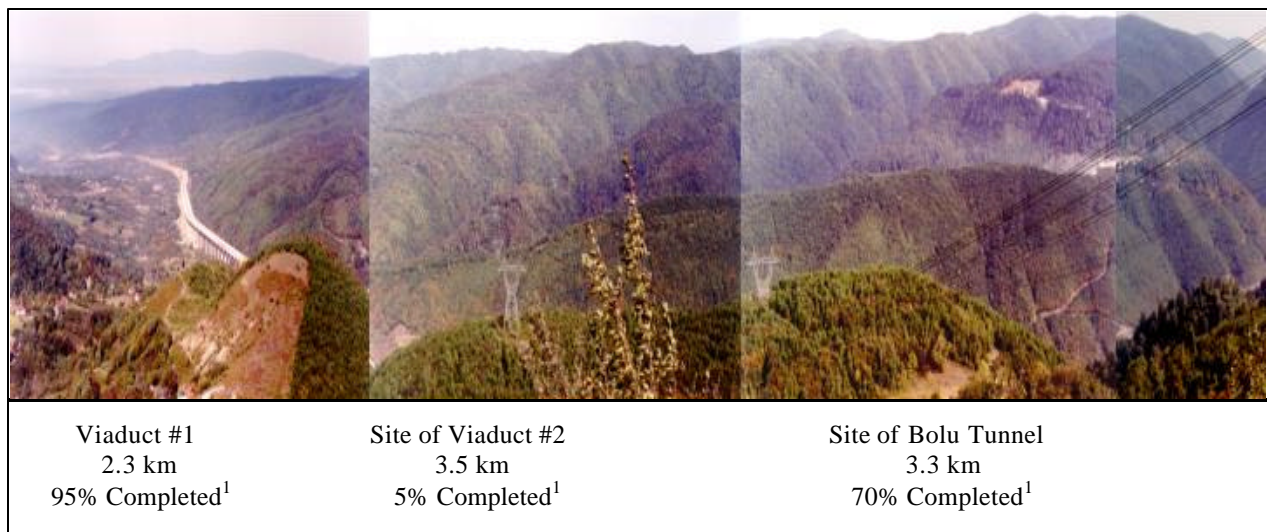


Figure 3. Damaged segment of the TEM.



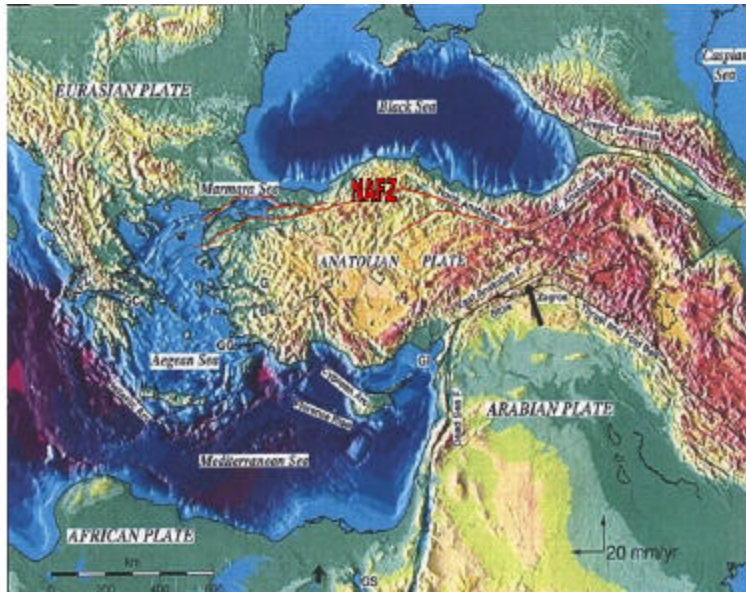
¹At the time of Duzce earthquake

Figure 4. General View of the Bolu Region.

The North Anatolian Fault Zone (NAFZ)

Except their timing, the occurrence of the Kocaeli and Duzce earthquakes on the NAFZ was no surprise. The NAF is the most prominent active fault zone, which runs across northern Turkey with an approximate length of 1300 km and a slip rate of 25 mm/yr.

Figure 5 shows the general tectonic setting of Turkey. The northwards motion of the Arabian plate against the Eurasian plate causes most of the ruptures along the NAF. Since the devastating 1939 Erzincan earthquake with its epicenter almost 1000 km east of Istanbul, earthquakes with a magnitude larger than 6.5 have occurred frequently along the NAF with their epicenters moving progressively westward towards Istanbul as indicated in 1997 by Stein et al. This has long caused much concern in Turkey and the recent Kocaeli earthquake with its close proximity to Istanbul has elevated these concerns.



<http://www.koeri.boun.edu.tr/earthqk/tectonic1.jpg>

Figure 5. Tectonic setting of Turkey.

The NAFZ has been studied as a collaboration effort by both Turkish and U.S. scientists for many years. In particular, U.S. scientists have been interested in the NAFZ because there is a strong similarity between the creep rate, total length, and energy release of both the North Anatolian and the San Andreas faults in California. Both faults have generated large magnitude earthquakes in the past.

The Trans European Motorway (TEM)

The Republic of Turkey with its 73 provinces and an estimated 65 million population provides a bridge between Europe and Asia. In order to achieve its economic development goals, Turkey spends a good third of all public investment on improving its transport infrastructure, by funding capital projects such as building roads and expanding the rail network, especially in the western part of the country.

During the last 10 years, Turkey has built 1,500 km of motorways with the major portion of the construction between Ankara and Istanbul, continuing to Europe (Figure 6). There is also 800 km of motorways under construction with the major portion from Ankara to the southern city of Adana. The TEM, the strip from Ankara to Europe, is designated as Route E80. This strip is built almost parallel to the NAFZ and includes a number of tunnels, viaducts, and many

underpasses as well as overpasses. It represents the major through route for the transportation of goods and other commerce from Asia to Europe. The KGM is responsible for the services and maintenance of the entire motorway in Turkey.

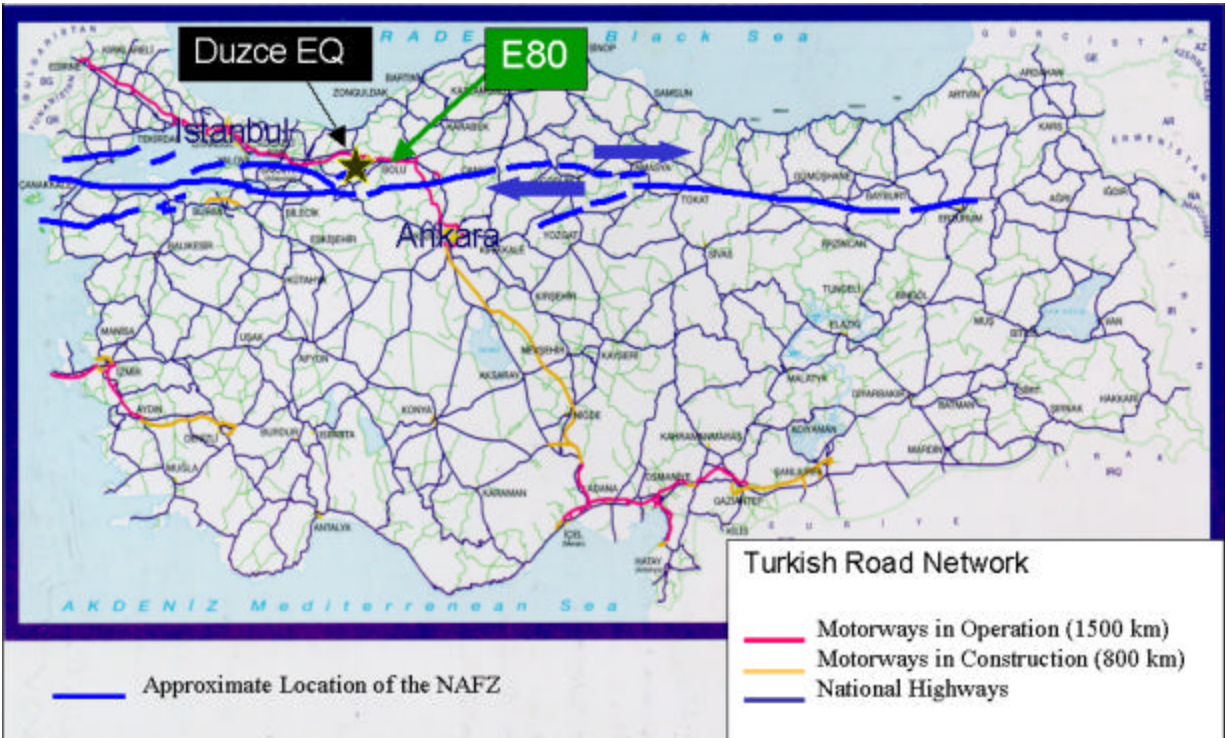


Figure 6. Turkish road network.

Sites Visited

1. Bolu Viaduct #1

Viaduct #1, with its dual 59 spans and 2.3-km structure was approximately 95% complete and was awaiting installation of expansion joints for completion of the project at the time of the November 12, 1999 Duzce earthquake (Figure 7). Its spans are 40 m in length and are comprised of seven lines of simply supported, prestressed concrete box girders seated on pot bearings with a stainless steel/polytetrafluoroethylene (PTFE)-slider interface. The deck slab acts continuously over 10 span segments. The viaduct's piers are single, octagonal, cast-in-place, hollow-core reinforced-concrete columns, 4.5 by 8.0 m in plan dimension, with heights varying from 10 m to about 49 m. They were designed and detailed to provide ductile behavior during earthquakes.

The viaduct had also incorporated an Energy-Dissipation Unit (EDU) system, which was installed on each pier cap to accommodate longitudinal thermal movements and to reduce any seismic forces through energy dissipation during a major event.



Figure 7. General view of Bolu Viaduct #1.

2. Bolu Bridge #2

Bridge #2 is an in-service, dual five-span, simply supported prestressed concrete box girder structure having a circular pier column and a very large horizontal radius of curvature (Figure 8). The spans sit on rectangular reinforced elastomeric bearing pads and EDUs similar to those used in Bolu Viaduct #1 to limit seismic response. The deck slab acts continuously over five spans.

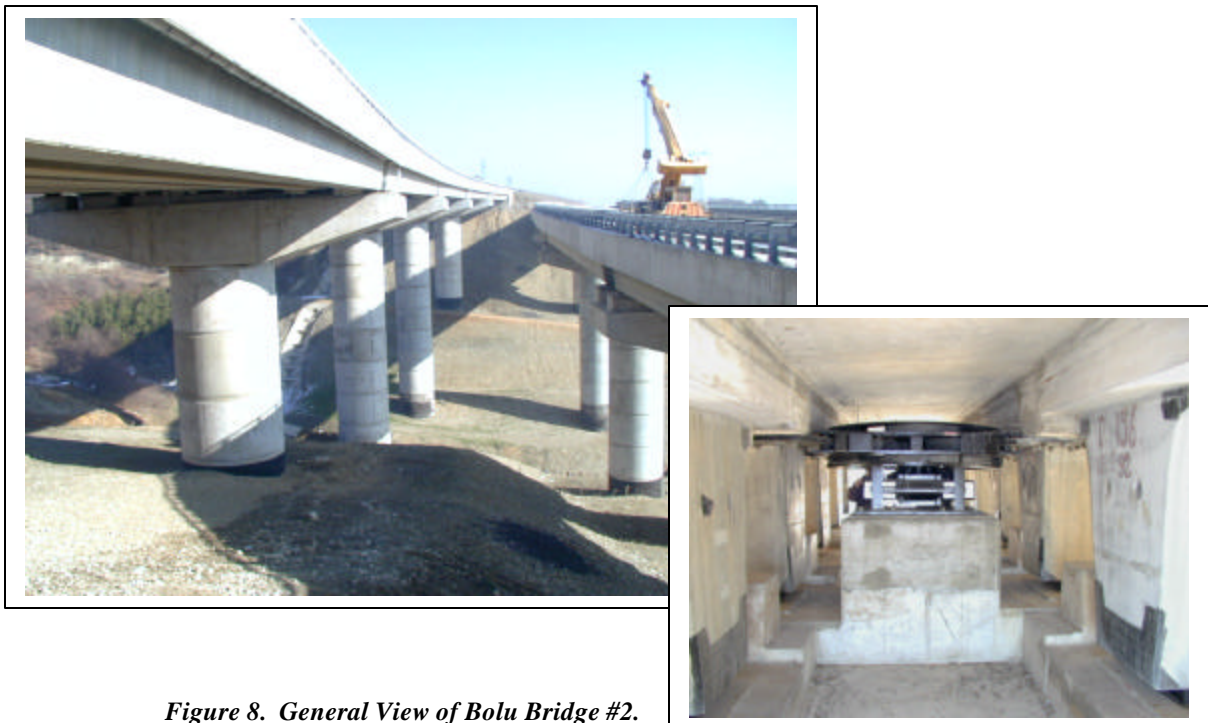


Figure 8. General View of Bolu Bridge #2.

3. Bolu Viaduct #2

Construction of Viaduct #2, a proposed 3.5-km dual structure, had just begun with the construction of the piled foundations at its eastern end. Construction was estimated to be less than 5% complete. Similar to Bolu Viaduct #1, Viaduct #2 was to incorporate the use of pot bearings, energy-dissipation units, cable restrainers, and ductile pier design to control seismic response.

4. Bolu Tunnel

At the time of the Duzce earthquake, excavation for 3.3-km twin Bolu bores was about 70% complete, with about 30% of the final liner system in place. Figures 9 and 10 show the tunnel portals at Elmalik (eastbound) and at Asarsuyu (westbound).



Figure 9. Bolu tunnel at the Elmalik portal.

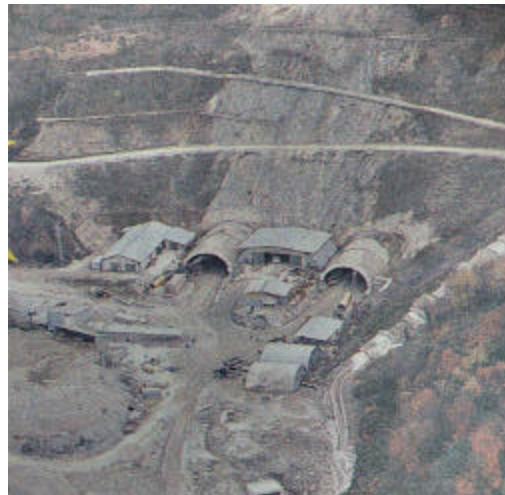


Figure 10. Bolu tunnel at the Asarsuyu portal.

Bolu Viaduct #1

Design Strategy

The design concept for Viaduct #1 involved the application of mixed criteria, using the 1990 American Association of State Highway and Transportation Officials (AASHTO) seismic design guidelines, coupled with the design of a hybrid isolation system based on Italian guidelines. The system is comprised of pot bearings with a Teflon-stainless steel sliding interface under each box girder and an EDU located at the center of each pier cap, which was bolted to a high reinforced-concrete pedestal on top of the pier cap and to the underside of the deck (Figure 11). The arrangement of EDUs for a 10-span simply supported segment of the viaduct is shown in Figure 12. Also, as shown in Figure 12, the deck slab is continuous over the intermediate supports.

The EDUs consist of C-shaped energy-dissipating steel elements that are referred to as “crescent moons” (in this report, they are referred to as “C-elements”) (Figure 11). These elements provide hysteretic behavior through yielding of the steel elements. In addition to the crescent moons, a

piston and a sliding unit are incorporated into the EDUs at the expansion joints and at the center pier of each 10-span continuous segment.



Figure 11. A pot bearing and an EDU unit.

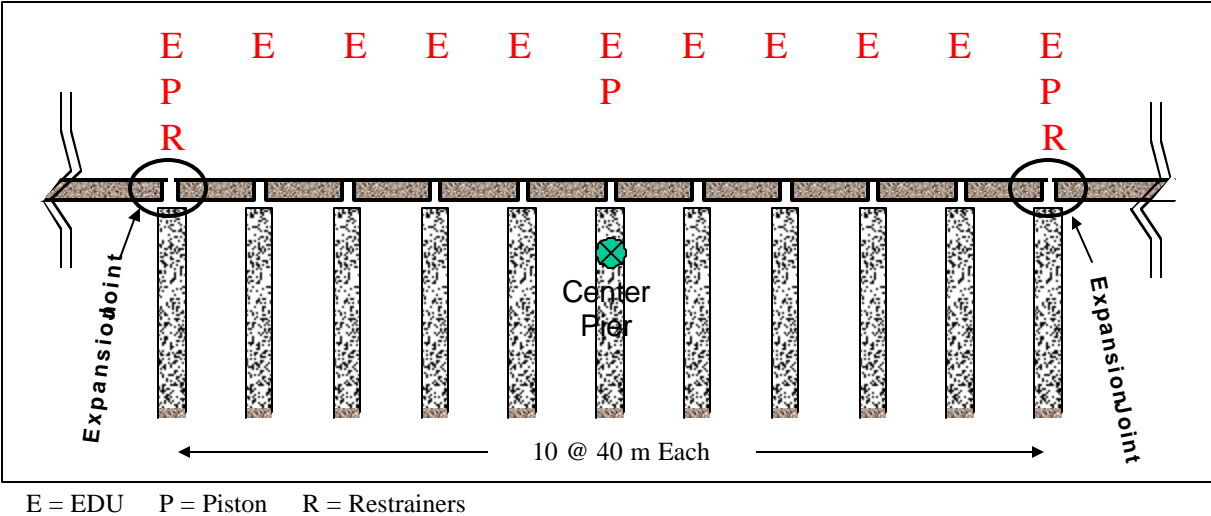


Figure 12. The arrangement of EDUs, with and without pistons and cable restrainers.

Cable restrainers were utilized at the expansion joints as a secondary line of defense to prevent the end girders from falling off their supports due to displacement beyond that assumed (Figure 13).



Figure 13. Cable restrainers at the expansion joint.

In summary, under normal environmental conditions (i.e., thermal expansion), the viaduct movement is provided by the PTFE-slider interface of the bearing, in conjunction with the sliding unit of the EDUs, which is controlled by the piston and is incorporated into the units.

However, during a design-level earthquake (acceleration of 0.4g), the piston would lock up (similar to a shock absorber) and would engage all of the EDUs on each 10-span continuous deck segment. This would dissipate the energy induced by the ground motion, which, in turn, would reduce the displacement response and the total force exerted on the substructure.

Figure 14 shows a typical force-displacement characteristic of an EDU at the ultimate displacement (± 480 mm). The enclosed area is the energy-dissipation capability of a unit that was designed for 40% of critical damping.

The team believed that a good seismic design philosophy had been selected, with an apparent ductile reserve capacity of the concrete piers for resisting earthquakes beyond the design-level earthquake.

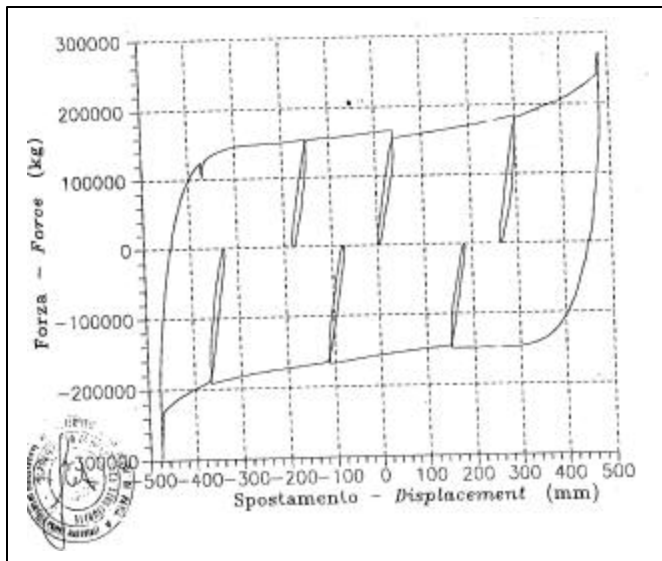


Figure 14. Actual testing results of an EDU at ultimate displacement (± 480 mm).

Field Observations

1. The surface fault trace was visible sporadically in the valley town of Kaynasli, where Viaduct #1 is located. Faulting caused major destruction of buildings, residential housing, and other facilities. The fault trace was also observed at Viaduct #1, where it intersected Pier #45 (eastbound), then continued between the two #46 piers before intersecting Pier #47 (westbound) as shown in Figure 15. Fault rupture movement, estimated to be about 2.5 to 3 m at this location, resulted in a rotation of nearly 13 degrees at Pile Caps #45 (eastbound) and #47 (westbound) about their vertical axes.

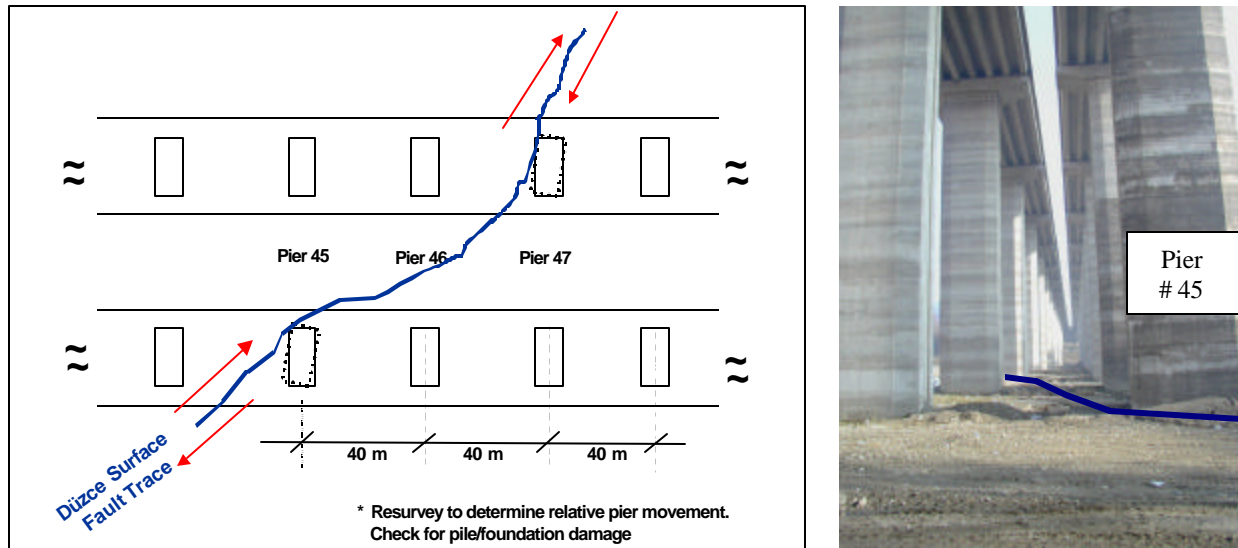


Figure 15. Fault trace at Viaduct #1.

2. Significant damage did occur to the EDUs and bearings from surface-rupture displacement and ground shaking, which then caused the superstructure girders to translate on their pier tables, narrowly avoiding total collapse (Figures 16 through 18).



Figure 16. Dislodged EDU, Pier #5.



Figure 17. Typical dislodgment of bearing systems.



Figure 18. End of fascia girder extending beyond pier table.

3. Shear keys or blocks used to control transverse girder movement, although severely damaged, have functioned as intended appear to (Figure 19).



Figure 19. Shear block damage (translational restraint).



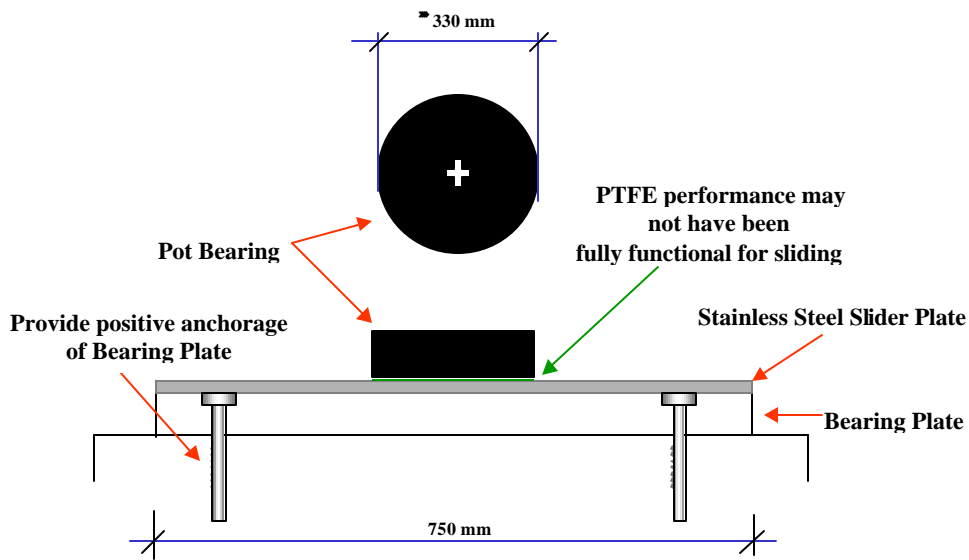
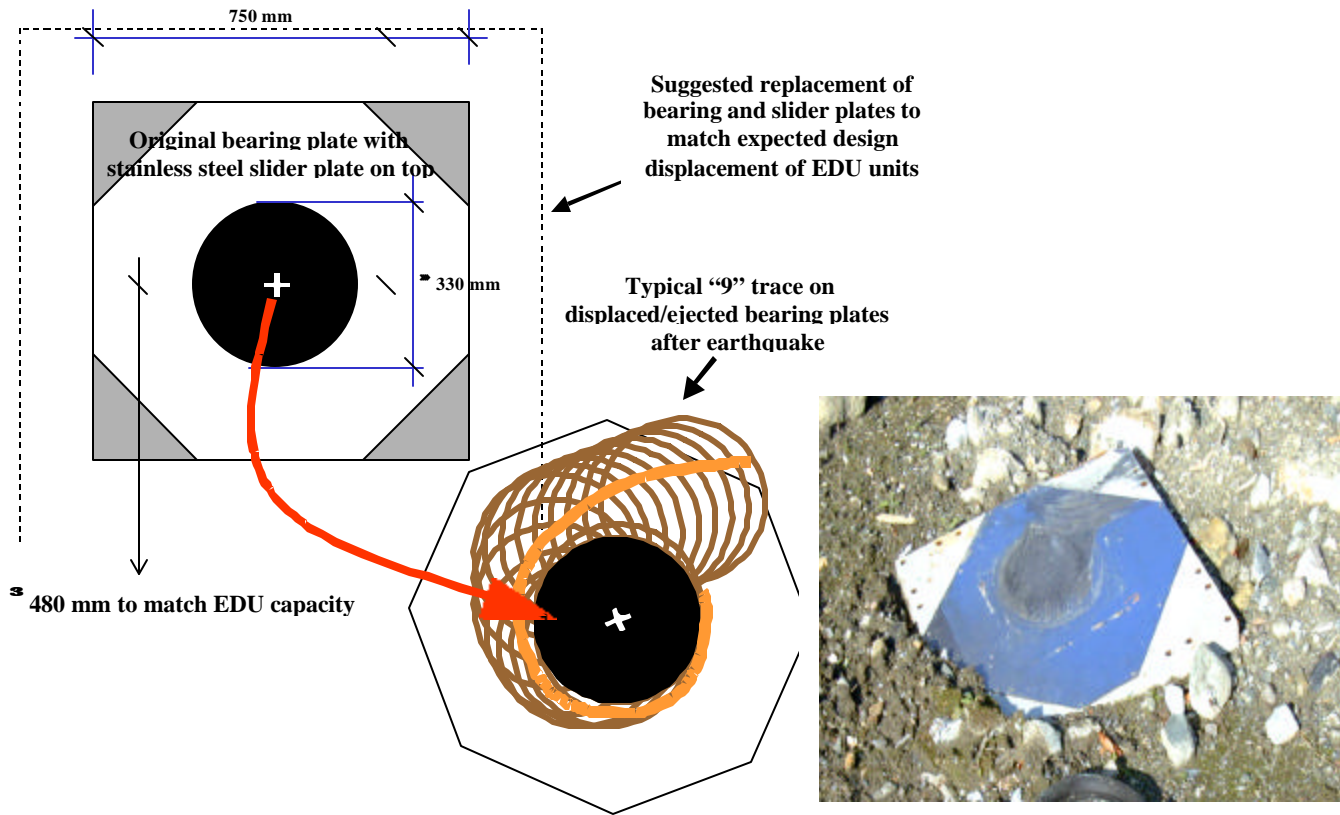
Damage Scenario

The following outline presents a damage scenario for Viaduct #1. It is based on the field observations made on November 30, 1999 and December 2, 1999.

1. The viaduct was first subjected to a low-frequency vibratory motion, which was then followed by a high-velocity impulse or "fling" resulting from the near-field effect. The surface fault trace was visible at Piers #45, #46, and #47 (Figure 15).
2. The fling caused the bearings to be ejected from underneath the box girders after the bearing sliding plate interface area was exceeded (Figure 17).
3. On some piers, especially those closer to the fault trace, the fling broke the epoxy bond of the bearing plates to both pier caps and the bottom flange of the box girders. Many of the bearing plates were found on the ground below.
4. On other piers, the stainless steel interface plates, which were epoxied to the bottom bearing plates, were protruding from the edge of the pier cap or were found on the ground below.
5. Almost all of the stainless steel interface plates had distinct scoring that resembled the number "9". The "9" trace may validate a scenario of large cyclic motion resulting from the fling effect (Figure 20). Also included in Figure 20 are the authors suggestions for remediation that were made at the time of the site investigation.
6. Upon the loss of the bearings from underneath the girders (and in some instances, the steel bearing plates, too), the superstructure then dropped approximately 5 cm to rest on the pier caps. That caused an excessive bending moment at the EDU connection to the deck, which resulted in the partial to total binding of the C-element ring plates (Figures 21 through 23). The binding action prevented the EDUs from functioning properly.
7. The fling effect possibly sheared off the connection between the EDU and its pier cap, as well as the connection to the deck. It is believed that the design of the EDU connections to the super- and substructure was based on the elastic limits of the C-element. The connections for the bearings plates were designed for a force level equal to the dynamic coefficient of friction of the PTFE-sliding bearing (4%).
8. It was also noted that the displacement capacity of the bearings (± 210 mm) was less than that of the EDU units (± 320 mm). Therefore, the EDUs would have never reached their optimum performance.
9. Most of the 10-span superstructure segments moved toward the west abutment. At the 10-span unit, which included Piers #45, #46, and #47 where the fault trace was visible, 3 of the girders slid off the cap of Pier #46 (Figure 18). This was possibly the result of rigid-body substructure motion to the east. The superstructure rested on PTFE-sliders, had a greater inertial mass relative to the substructure, and, therefore, was unable to follow the pier's movement. At the same time, the EDUs were probably not able to control the excess superstructure displacement if they were not functional after the initial velocity impulse. Whether the piers, the deck, or both moved can be better determined after a final and precise survey of the bridge is made.

10. It appeared that the piers were not subjected to many flexural cycles of motion as indicated by the lack of pier flexural cracking. The only hairline flexural-induced cracking noted was at Piers #35 and #36. Upon their sudden failure, the bearings and EDUs behaved as a fuse, apparently decoupling the substructure from the high-impulse load due to surface-fault rupture at the site. This fuse-type behavior points out the effectiveness of the isolation approach in protecting substructure elements.

In summary, significant superstructure movements relative to the substructure caused damage to the bearings and EDUs on Viaduct #1. However, from a technical point of view, the viaduct performed satisfactorily. During the Duzce earthquake, which produced much larger forces than the design earthquake, collapse did not occur.



Recommendation: Expand to 1000 mm in redesign, but check pot bearing / EDU system performance for maximum credible earthquake

Figure 20. Viaduct #1 bearing damage scenario (based on the site review on November 30, 1999).



Figure 21. Bearing failure.



Figure 22. EDU failure.

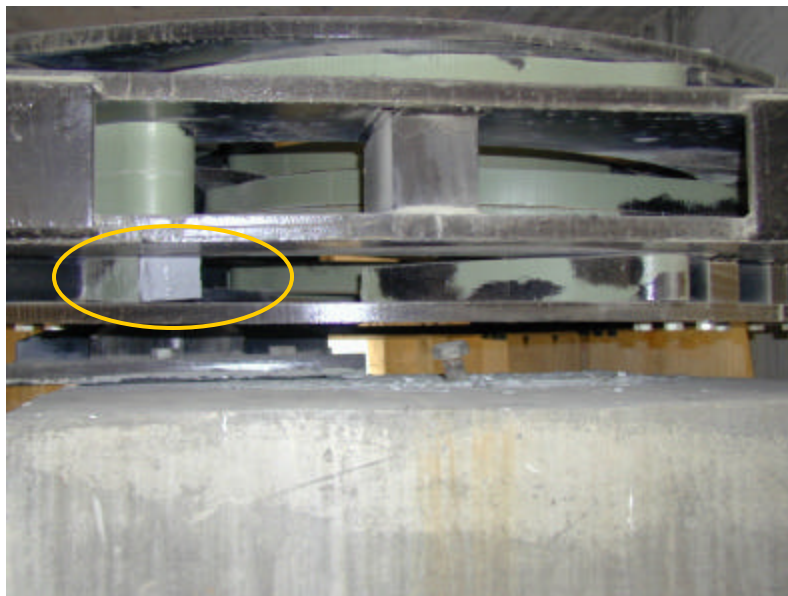


Figure 23. Fractured EDU C-element

Bolu Viaduct #2

Design Strategy

The design concept for Viaduct #2 is similar to that of Bolu Viaduct #1. It is designed to incorporate a hybrid isolation system that is comprised of a pot bearing with stainless steel PTFE-sliding interface under each box girder and an EDU device at each pier. Only 5% of Viaduct #2 was constructed at the time that this report was written.

Bolu Bridge #2

Field Observations

1. Moderate structural damage occurred to the concrete box girders of Bridge #2. The west end of the eastbound span translated approximately 3.5 in (88.9 mm) to the north relative to the west abutment, as evidenced by the misalignment of lane striping at the west abutment (Figure 24).



Figure 24. Translation of the eastbound span at the west abutment.

2. Examination at the abutment seat revealed a set of well-proportioned, steel-reinforced, rectangular elastomeric bearing pads (Figure 25) and an EDU device that had functioned properly during the Duzce Earthquake (Figure 26). One C-element had compressed to a 23.5-in (596.9-mm) opening from center of pin to center of pin, while the other C-element extended to an opening of 31 in (787.4 mm). Markings on a bearing plate indicated that the 12-in by 27.5-in by 4.5-in- (304.8-mm by 698.5-mm by 114.3-mm-) thick bearing pad had translated about 6.5 in (165.1 mm) to the north and about 3.75 in (95.3 mm) to the west. Movement of the elastomeric bearings allowed the EDU to function and dissipate energy as conceptually designed.
3. Inspection of the eastbound span at the first pier table of the western abutment indicated that the bearings allowed the EDU to function properly. It was also noted that one of the anchorages of the EDU brackets that was attached to the superstructure appeared to be at incipient failure, i.e., cracking of the concrete at the EDU anchorage point was noted (Figure 27).



Figure 25. Well-proportioned, steel-reinforced elastomeric bearing pad showing evidence of translation.



Figure 26. Flaked-off paint of an EDU C-element that had functioned properly.

In addition, the grade of the superstructure resulted in a natural 2-in (50.8-mm) differential offset between the bracket attachments between the spans. This differential distance allows a naturally occurring, biased moment or twisting to occur across the EDU, which could bind the top and bottom rings, thus locking the C elements and rendering the EDU inoperative.

4. The stable performance of the well-proportioned, steel-reinforced elastomeric bearing pads and bearing plates with sufficient sliding capacity, in all likelihood, allowed the EDU to function, although any additional shaking could have caused the positive attachment of the EDU top brackets to the superstructure to fail. When using isolation/EDU systems, it is imperative that the independent units (bearings, plates, and EDU) be designed to act as a system.



Figure 27. Incipient failure of EDU anchorage point.

Bolu Tunnel

Design Strategy

A typical cross-section of the tunnel is shown in Figure 28. Its construction is based on the New Austrian Tunneling Method (NATM). The tunnel consists of three layers (from outside inwards) of shotcrete, reinforced concrete, and, finally, an unreinforced-concrete layer. The complexity of the site forced the designers to consider four options for construction:

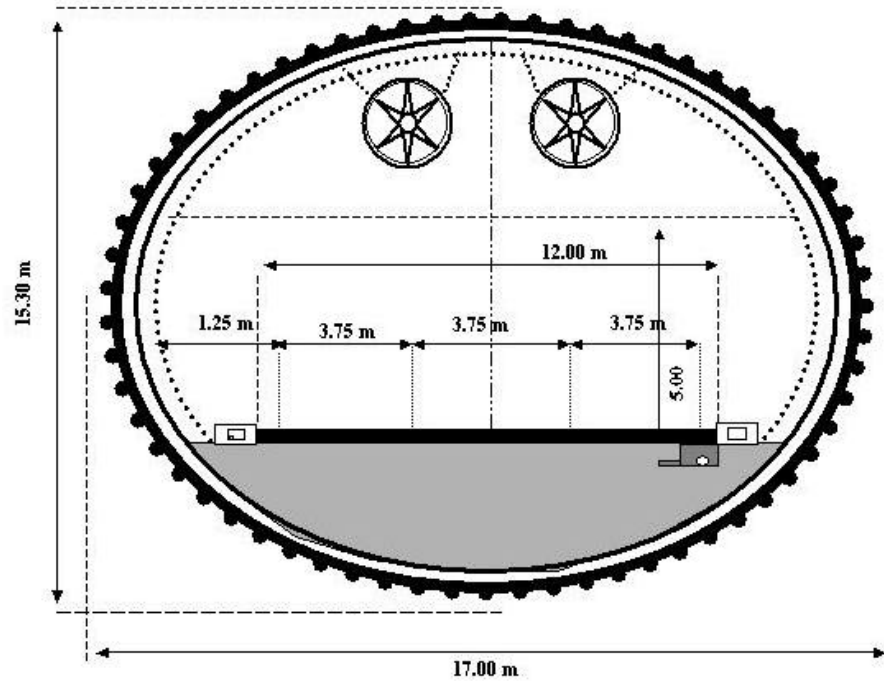


Figure 28. Cross-section profile.

Option 1 was to advance by blasting, followed by shotcreting over rock. Option 2 was similar to option 1; however, a thicker shotcrete section was required. Due to the continuous deformation of the clay deposit at sections of the tunnel, a third option was considered. This option required 45 cm of shotcrete, 60 cm of intermediate reinforced concrete, and, finally, a 60-cm unreinforced-concrete lining.

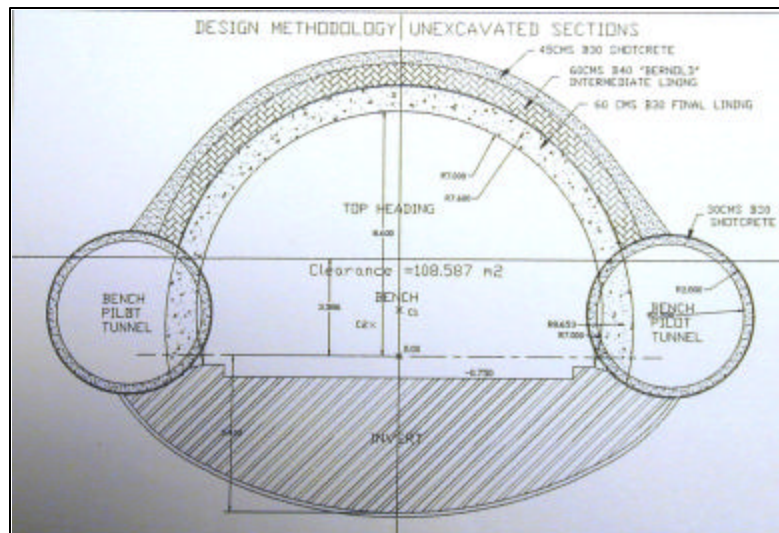


Figure 29. Option 4 tunneling technique.

Option 4, as shown in Figure 29, was planned for the worst condition, since there was evidence of soil squeezing and also sinking of the tunnel due to extremely soft soil. In this option, two pilot bench tunnels with a radius of 2.5 m were excavated along the sides of the tunnel for rigidity and to stabilize the tunnel movement. The pilot bench tunnels were later filled with concrete. In bridge terms, these tunnels act similarly to bridge abutments.

The seismic design for the tunnel was based on experience and judgment. An Effective Peak Acceleration (EPA) of 0.4g was used in design, which corresponds to a return period of about 500 years.

Field Observations

1. A very brief visual inspection of the Bolu tunnels was made on December 2, 1999. The inspection consisted of driving through both bores, from the Elmalik portal to the collapsed sections, approximately 300 m from the portal entrance, with limited time spent at the face of the collapse and in the structurally incomplete segment leading to the collapse. The incomplete section had only a shotcrete liner system in place.
2. Complete closure of both tunnel bores was noted about 200 to 300 m from the Elmalik portal entrances (Figure 30).

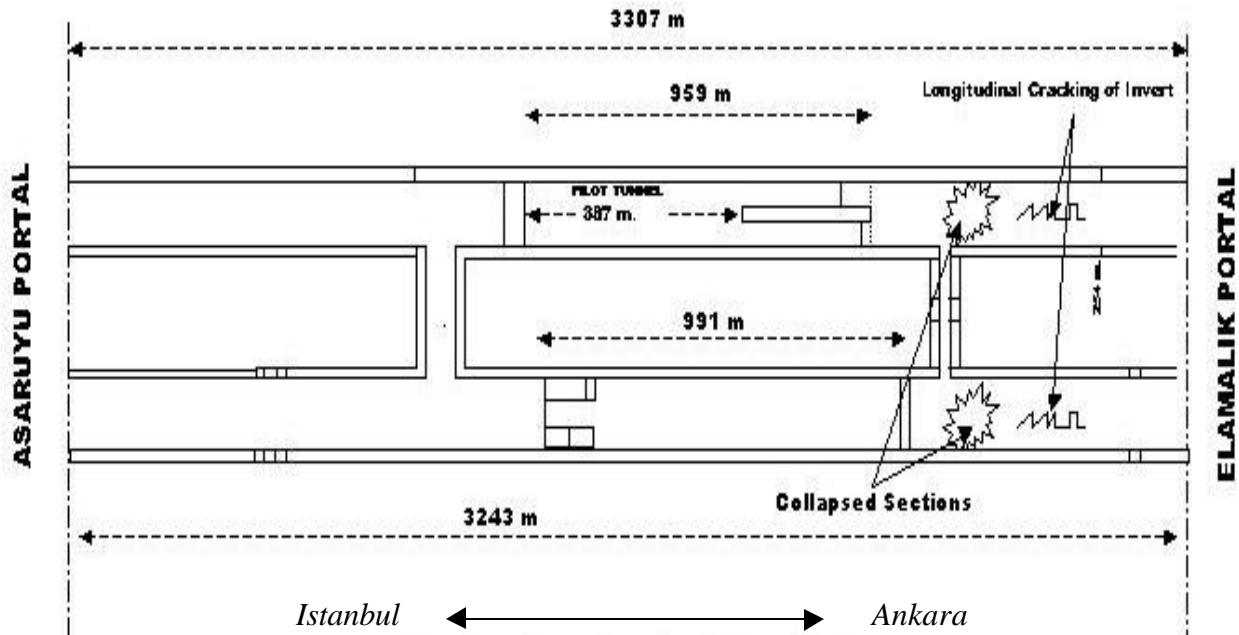


Figure 30. Approximate location of Tunnel collapse.

3. The collapses occurred in a section of tunnel passing through a clay/weak rock zone where a temporary shotcrete lining system was in place (Figures 31 and 32). The collapses occurred about 50 to 75 m beyond a structurally complete tunnel liner system.
4. Severe shotcrete spalling was noted between sets and at the sets along the tunnel wall (Figures 33 and 34).

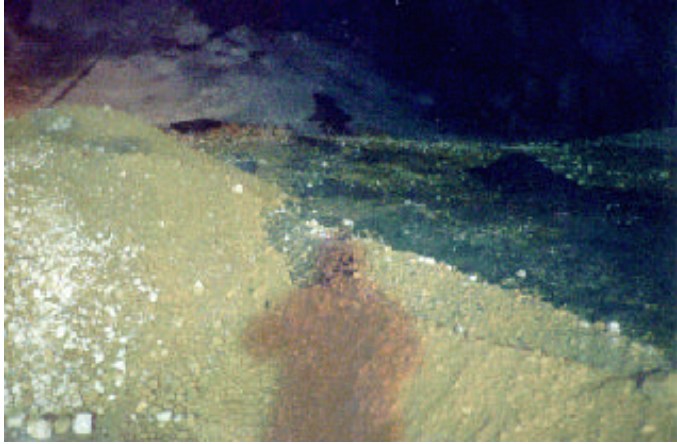


Figure 31. View looking head-on at the collapse of the westbound tunnel.



Figure 32. View looking at the collapse of the eastbound tunnel.



Figure 33. Spalled shotcrete liner segment.



Figure 34. Spalled shotcrete at sets.

5. One-millimeter-wide longitudinal and radial cracks were observed in the structurally complete reinforced-concrete liner (Figures 35 and 36).
6. Cracking of the reinforced-concrete utility box beams was also noted (Figures 37 and 38).



Figure 35. Longitudinal cracking of concrete liner



Figure 36. Radial cracking of concrete liner



Figure 37. Utility box beam cracking.



Figure 38. Completed concrete liner showing utility box beam.

9. Longitudinal cracking along a segment above the tunnel invert, near the collapsed face, was noted (Figure 39). It was reported by the consultant that the invert had heaved upwards as much as 1 m.



Figure 39. Longitudinal cracking above invert.

Summary/Conclusions

- The FHWA team inspected the roadway alignment and the physical condition of Bolu Viaducts #1 and #2, and Bolu Bridge #2. Also, Bolu tunnel damage was viewed from the Elmalik entrance westward to the collapse in both tunnels.
- The Duzce earthquake caused considerable damage to the superstructure of Viaduct #1 and to the Bolu tunnel due to the close proximity of fault rupture (near-fault effect). A surface-fault trace was visible between a segment of Viaduct #1 piers and evidence of high-velocity impulses was observed from the earthquake records and at the sites.
- The stations at Duzce and Bolu, 30 km apart, recorded PGAs of 1.0g and 0.8g, respectively. Therefore, it is reasonable to assume that Bolu Viaduct #1 (which was not instrumented), located between these two stations, experienced a PGA in excess of 0.4g, its design value.
- Significant damage did occur to the EDUs and bearings of Bolu Viaduct #1 from surface rupture displacements and ground shaking, which then caused the superstructure girders to translate on their pier tables, narrowly avoiding total collapse.
- The positive connections of many EDUs to the superstructure and pier cap of Bolu Viaduct #1 were sheared off after the initial high-velocity impulse.
- Shear keys or blocks used to control transverse girder movement of Bolu Viaduct #1, although severely damaged, appear to have functioned as intended.
- Moderate structural damage occurred to the concrete box girders of Bolu Bridge #2. The west end of the eastbound span translated approximately 3.5 in (88.9 mm) to the north relative to the west abutment.
- Although the bearing pads on Bolu Bridge #2 had translated about 6.5 in (165.1 mm) to the north and about 3.75 in (95.3 mm) to the west, there was no significant damage to the EDUs and bearings. However, cracking of the concrete was noted at one of the anchorages of the EDU brackets that was attached to the superstructure.
- Complete closure of both Bolu tunnel bores was noted about 200 to 300 m from the Elmalik portal entrances. The collapses occurred in a section of tunnel passing through a clay/weak rock zone where a temporary shotcrete lining system was in place. Severe shotcrete spalling was noted between sets and at the sets along the tunnel wall.

In summary, the close proximity of the fault rupture to the Bolu structures caused significant superstructure movement relative to the substructure, which resulted in severe damage to bearings and EDUs, in particular, on Bolu Viaduct #1. However, from a technical point of view, the viaduct performed satisfactorily. During the Duzce

earthquake, which produced much larger forces than the design earthquake, collapse did not occur. Also, due to the similarities between the NAF zone and the San Andreas fault, much can be learned by the earthquake engineering and seismological communities in the United States from the damage inflicted on the bridges by the November 12, 1999 Duzce earthquake. The near-fault effect, and the behavior of the EDUs and their positive connection to super- and substructures are just a few of the factors that can help others in designing and retrofitting bridges to resist future NAF zone-type seismic activity.

FHWA Team Members:

James D. Cooper, P.E., Technical Director, Bridge R&D, Turner-Fairbank Highway Research Center, McLean, VA.

Hamid Ghasemi, Ph.D., Research Structural Engineer, Bridge R&D, Turner-Fairbank Highway Research Center, McLean, VA.

Roy A. Imbsen, Ph.D., President, Imbsen & Associates, Inc., Sacramento, CA.

Turkish Team Members:

Hasan Piskin, Director, Motorway Bridge Division, General Directorate of Highways, Ankara, Turkey

Fulya Inal, Chief Engineer, Motorway Bridge Division, General Directorate of Highways, Ankara, Turkey

Azmi Tiras, Chief Construction Engineer, Motorway Bridge Division, General Directorate of Highways, Ankara, Turkey

Acknowledgements

The FHWA team would like to express its sincere appreciation to KGM Director General, Mr. Dincer Yigit, for his outstanding courtesy, professionalism and support. Also, special thanks to Mr. Hasan Piskin, Ms. Fulya Inal, and Mr. Azmi Tiras for their kind assistance during the investigation team's visit to Turkey. They have provided invaluable information during the team's visit and through follow up correspondence.

Other individuals who have helped in facilitating the team's visit are:

General Directorate of Highways (KGM)

Mr. Zeki Numanoğlu

Mr. Uzcan Erol

Mr. Recai Yilmaz

Yuksel & Rendel

Mr. Saik Tokgokoglu

Mr. Robin Miles

Mr. Paul Sanders

Mr. M W C Taylor

Mr. Mehmet Cilingir

Dr. Chris Menkiti

The team also wishes to give special thanks to the FHWA Office of International Programs, in particular Mr. King Gee and Mr. James Hansen whose strong support made this very important trip possible.

References:

Stein R.S., Barka, A.A. and Dieterich, J.H., "Progressive failure on the North Anatolian fault since 1939 by earthquake stress triggering," *Geophysical Journal International*, Vol. 128, 594-604, 1996.

Kocaeli Earthquake, Turkey, [on-line], Bogazici University Kandilli Observatory & Earthquake Research Institute, 1999 - <http://www.koeri.boun.edu.tr/earthqk/earthqk.html>

Duzce Earthquake, Turkey, [on-line], Bogazici University Kandilli Observatory & Earthquake Research Institute, 1999 - <http://www.koeri.boun.edu.tr/earthqk/earthqk.html>